

Endosome motility defects revealed at super-resolution in live cells using HIDE probes

Aarushi Gupta¹, Felix Rivera-Molina², Zhiqun Xi², Derek Toomre^{2*}, Alanna Schepartz^{1,3,4*}

¹Department of Chemistry, Yale University, New Haven, CT 06520, USA

²Department of Cell Biology, Yale University School of Medicine, New Haven, CT 06510, USA

³Department of Molecular, Cellular, and Developmental Biology, Yale University, New Haven, CT 06520, USA

⁴Current address: Department of Chemistry, University of California, Berkeley, CA 94720, USA

***Authors to whom correspondence should be addressed:** schepartz@berkeley.edu and derek.toomre@yale.edu

List of Supplemental Figures and Movies

Supplementary Figure 1: Confocal and STED Microscopy with DiIC₁₆(3)

Supplementary Figure 2: Localization of DiIC₁₆-SiR (and DiIC_{16'}-SiR) is dependent on two-step labeling and the presence of both IEDDA partners

Supplementary Figure 3: Minimal galectin recruitment under various conditions shows lack of endosome damage with DiIC₁₆-SiR and DiIC_{16'}-SiR

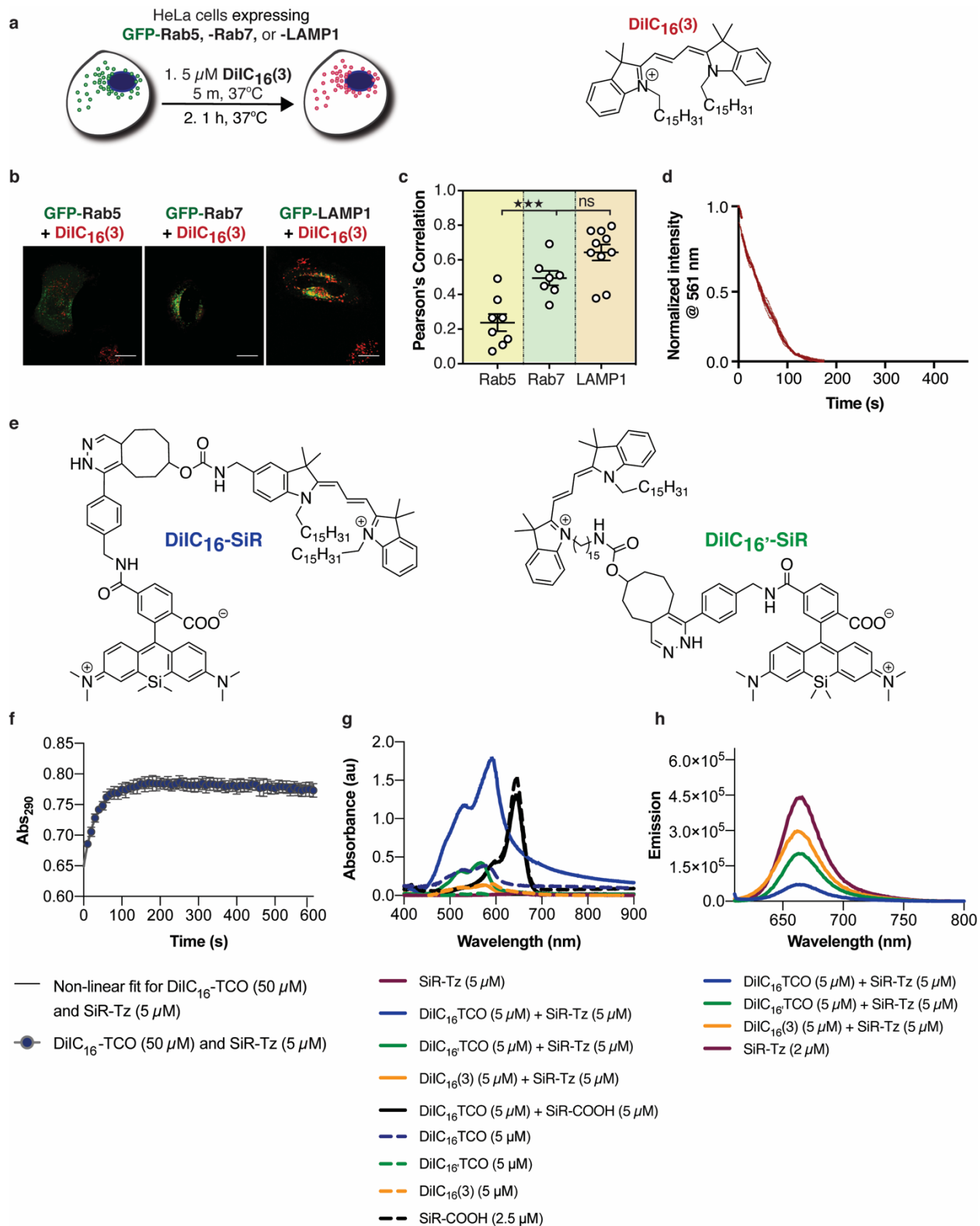
Supplementary Figure 4: EGFR trafficking and DiIC₁₆-SiR imaging with HeLa cells expressing GFP-Rab7

Supplementary Figure 5: Long-term imaging with DiIC₁₆-SiR, DiIC_{16'}-SiR and Rab7-SiR and effects on cell viability

Supplementary Figure 6: Endosome tracking in WT fibroblasts with confocal and STED microscopy

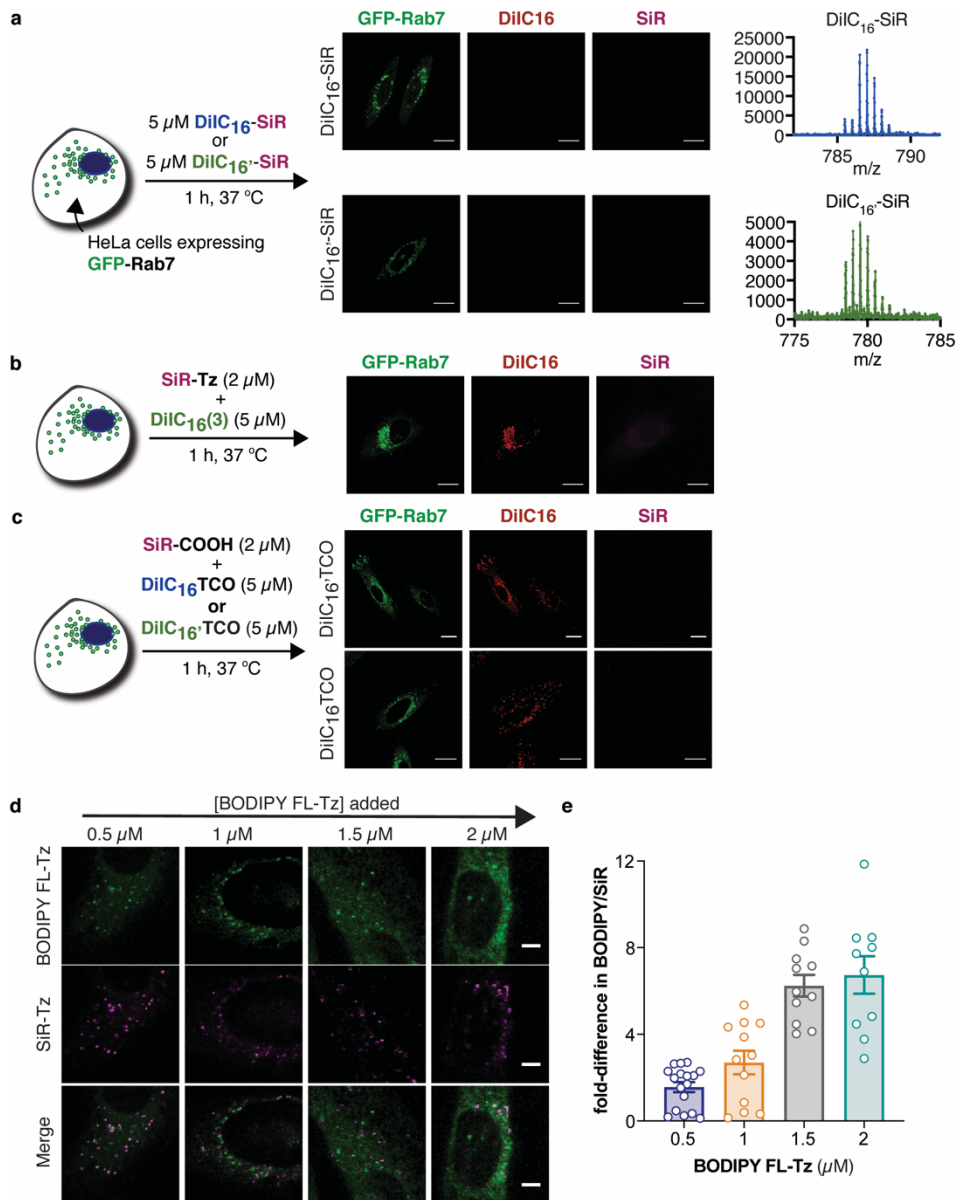
Legends for Supplementary Videos 1-7: HeLa cells and GM05399, GM23945, GM18453, GM03123 and GM18388 fibroblasts

Supplementary Note: Synthesis and characterization of DiIC₁₆TCO and DiIC_{16'}TCO



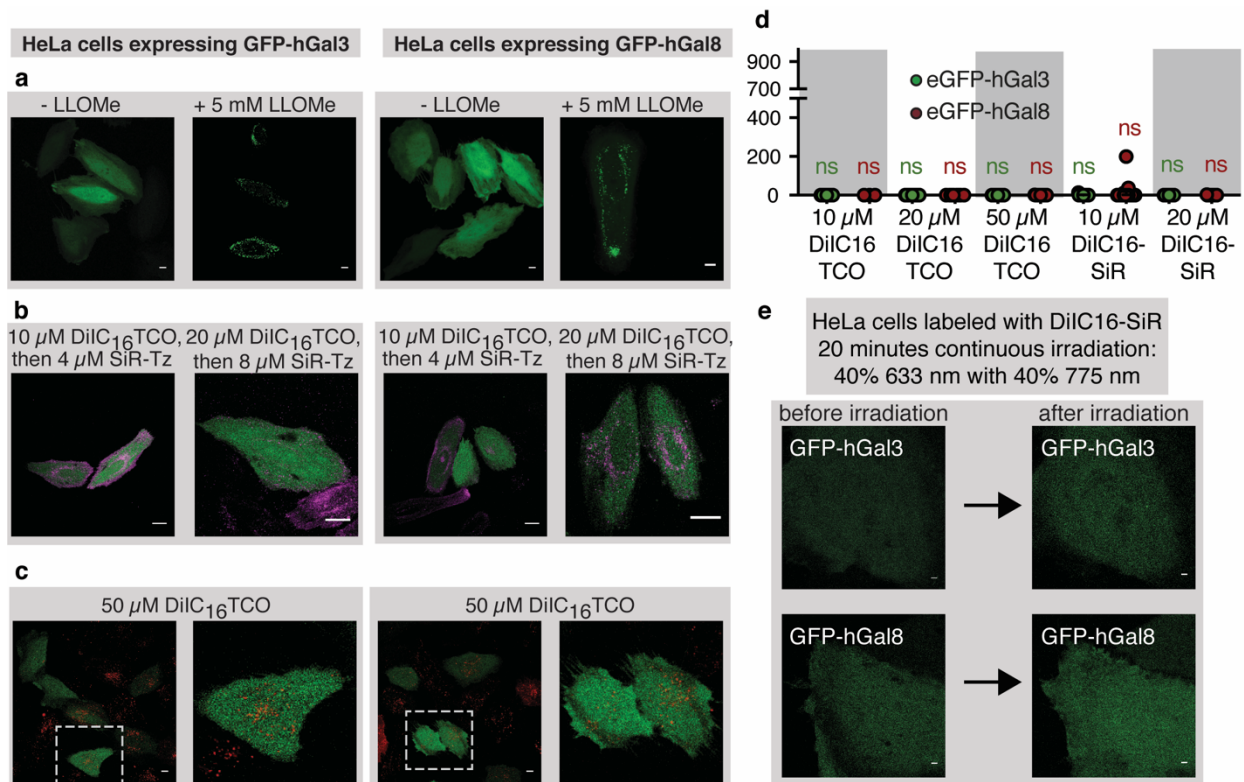
Supplementary Figure 1. Localization of DiIC₁₆(3) to endocytic organelles. (a) Labeling of HeLa cells with DiIC₁₆(3). Cells were treated with 5 μM DiIC₁₆(3) for 5 minutes, followed by a 1-

hour chase in DMEM (pH -) at 37°C. (b) Laser-scanning confocal microscopy of HeLa cells expressing GFP-Rab5, GFP-Rab7, or Lamp1-GFP and treated with DiIC₁₆(3), scale bars: 20 μM. (c) Average Pearson's correlation coefficient (PCC) representing the colocalization of DiIC₁₆(3) with endosome markers. Each PCC value was calculated from 8 discrete cells, and the average is shown as the midpoint. Experiment was repeated 3 times independently with similar results, error bars represent the s.e.m. (***p < 0.001, **p < 0.01, *p < 0.05, and not significant (ns) for p > 0.05, one-way ANOVA followed by Tukey's multiple comparisons test). (d) Photobleaching curve of DiIC₁₆(3) with STED microscopy. Data represents average of 3 individual cells with s.e.m. shown. (e) Chemical structures of DiIC₁₆-SiR and DiIC₁₆-SiR HIDE probes. (f) Kinetics of reaction between DiIC₁₆TCO and SiR-Tz in DPBS; 5 μM SiR-Tz was incubated with and without 50 μM DiIC₁₆TCO and the absorbance at 290 nm was monitored every 10 seconds. The increase in absorbance at 290 nm was fit to a pseudo-first order rate equation, which was then used to calculate a second-order rate constant. The second-order rate constant was $605 \pm 78 \text{ M}^{-1} \text{ s}^{-1}$, which corresponds to a reaction half-life of $23 \pm 4.5 \text{ s}$. Experiment was repeated 3 times independently with similar results, center values represent the mean and error bars represent the s.e.m. (g) Absorbance and (h) Fluorescence spectra of DiIC₁₆-SiR and DiIC₁₆-SiR in DPBS (pH 7.4). DiIC₁₆(3) does not emit in the range shown in (h). Solutions containing 5 μM DiIC₁₆TCO, DiIC₁₆TCO or DiIC₁₆(3) in Dulbecco's Phosphate Buffered Saline were incubated with 5 μM SiR-Tz or SiR-COOH at 37°C for 10 minutes. Absorbance was measured on a Beckmann Spectrophotometer and emission monitored using a TCSPC TD-Fluor Horiba Fluorolog 3 Time Domain Fluorimeter; both were measured at room temperature. Both absorbance and fluorescence were measured once.

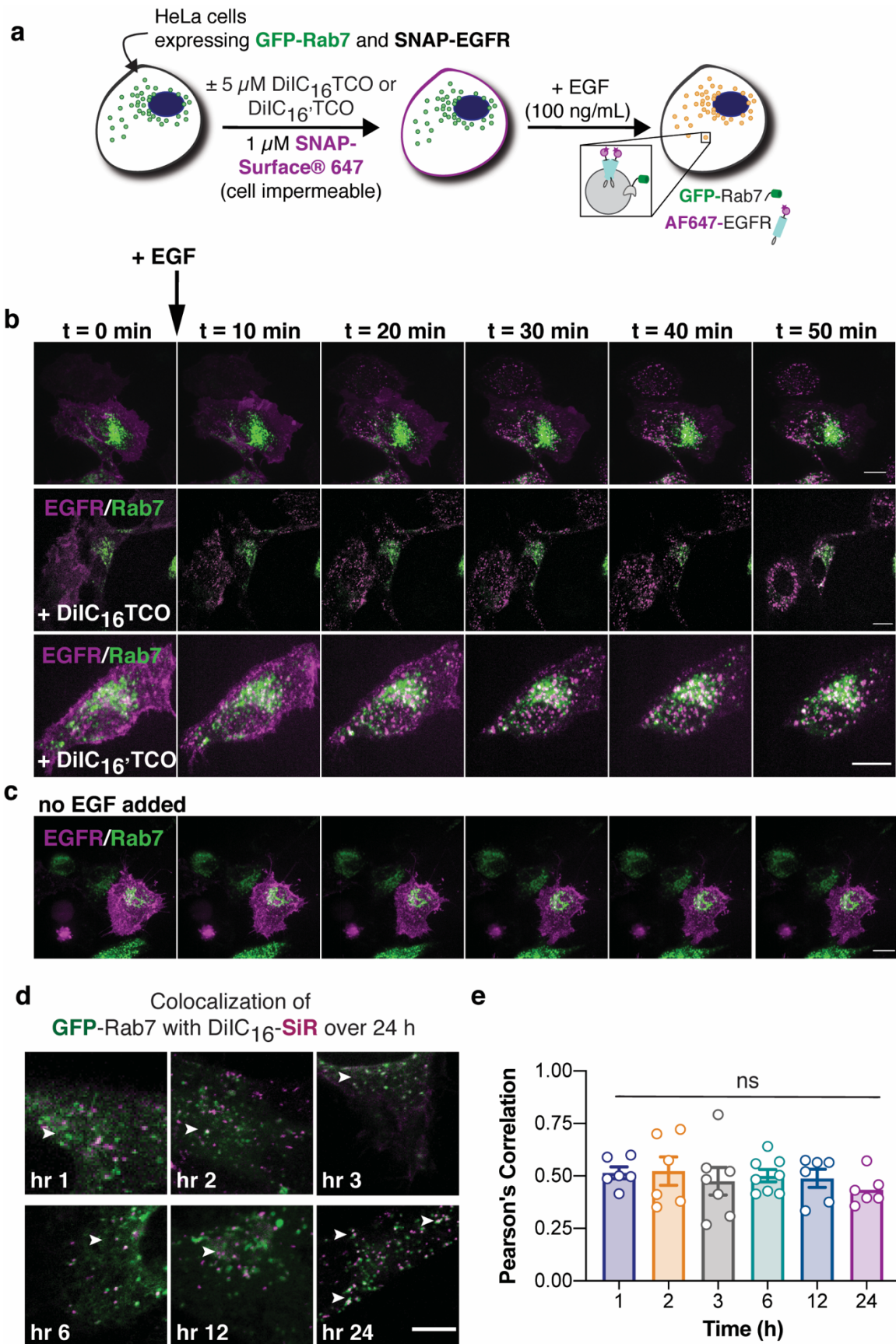


Supplementary Figure 2. Localization of DiIC₁₆-SiR (and DiIC₁₆'-SiR) is dependent on two-step labeling and the presence of both tetrazine ligation partners. (a) Pre-formed DiIC₁₆-SiR does not localize to late endocytic compartments in HeLa cells. 5 μ M of each component were incubated together for 30 minutes at 37°C. The resulting adduct (characterized by LCMS) was then diluted with DPBS with 1% BSA and added to HeLa cells for 10 minutes at 37°C and imaged by confocal microscopy. Experiment was repeated 2 times independently with similar results, scale bar: 20 μ m. (b) HeLa cells incubated with DiIC₁₆TCO or DiIC₁₆'-TCO and SiR-COOH show no SiR fluorescence. Experiment was repeated 2 times independently with similar results, scale bar: 10 μ m (c) HeLa cells labeled with DiIC₁₆(3) and SiR-Tz show no SiR

fluorescence. Experiment was repeated 2 times independently with similar results, scale bar: 10 μm . (d) HeLa cells were incubated with DiIC₁₆TCO and SiR-Tz as described in the Methods section: 5 μM DiIC₁₆TCO followed by 2 μM SiR-Tz. Immediately following SiR-Tz incubation, between 0.5 and 2 μM BODIPY FI-Tz was added to react with the remaining DiIC₁₆TCO, and the cells were imaged with laser-scanning confocal microscopy (scale bar: 10 μm). (e) Approximately 50% of DiIC₁₆-TCO reacts with SiR-Tz in live cells. The intensity of SiR and BODIPY (in cells from (d)) were independently measured and divided to yield the ratio between BDP/SiR fluorescence. This value (BDP/SiR fluorescence) for each concentration of BODIPY was plotted and shows that approximately 1.5 μM of BODIPY FL-Tz is sufficient to react with remaining DiIC₁₆TCO. $n = 6$ biologically independent cells for each condition, centerline and error bars represent average with s.e.m.

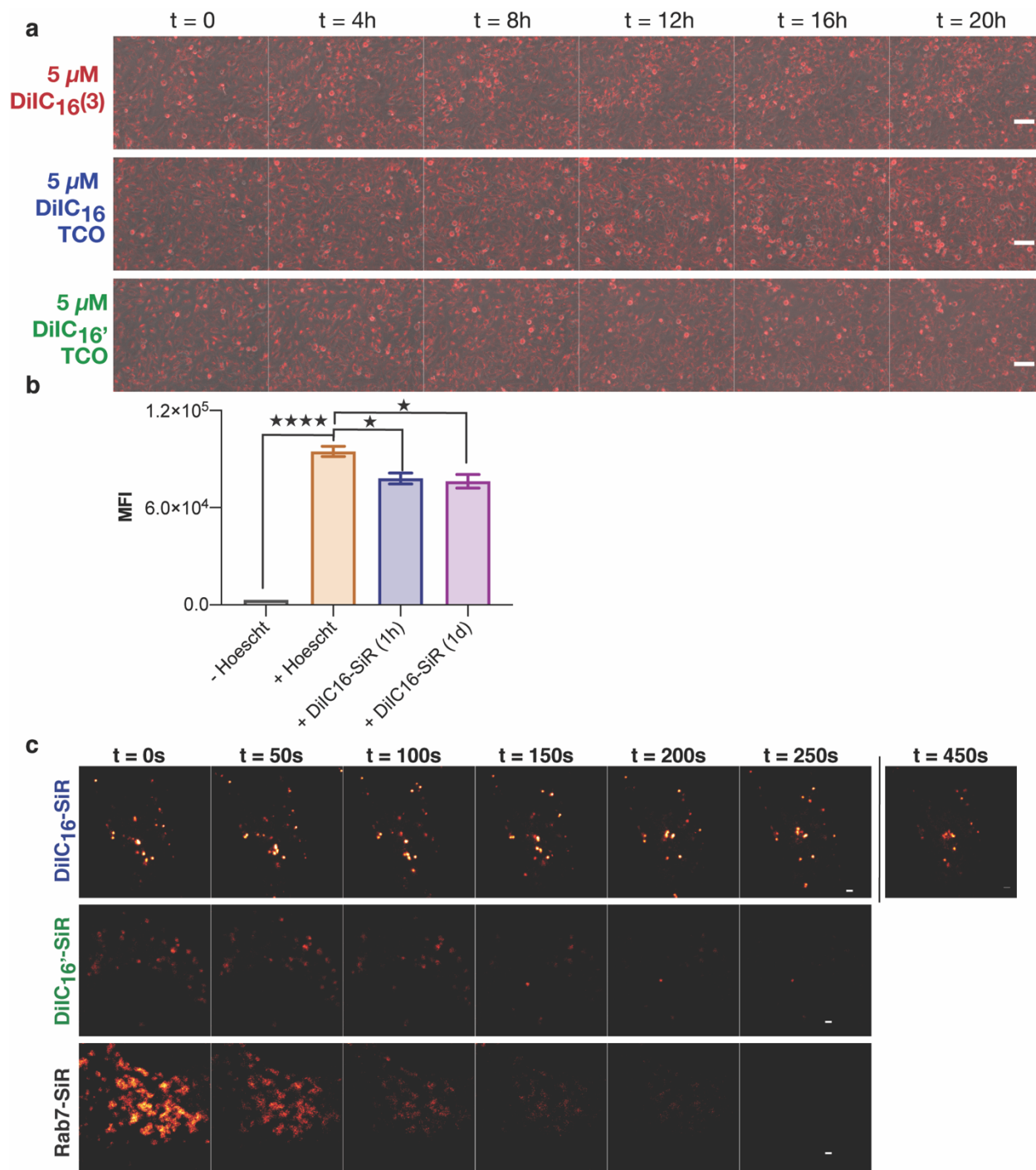


Supplementary Figure 3. Minimal galectin recruitment under various conditions shows lack of endosome damage with DiIC₁₆-SiR and DiIC₁₆-SiR. (a) Representative laser-scanning confocal microscopy of eGFP-hGal3 and eGFP-hGal8 with and without 5 mM endosmolytic reagent LLOMe (scale bar: 10 μ m). Experiment was repeated 2 times independently with similar results. (b) Increasing concentrations of DiIC₁₆TCO and SiR-Tz does not lead to hGal3 or hGal8 recruitment, as quantified by GRC. (c) Increasing concentrations of DiIC₁₆TCO to 50 μ M does not lead to detectable galectin recruitment. Experiment was repeated 2 times independently with similar results, scale bar: 10 μ m. (d) Galectin recruitment coefficients for all saturating conditions with DiIC₁₆TCO and/or SiR-Tz. Representative microscopy images represent average GRC values from $n = 7$ biologically independent samples for DiIC₁₆-SiR or DiIC₁₆-SiR with each galectin protein, error bars represent s.e.m. (not significant (ns) for $p > 0.05$, one-way ANOVA). All comparisons made to untreated cells expressing eGFP-hGal3 or eGFP-hGal8. (e) STED irradiation for 20 minutes in DiIC₁₆-SiR-labeled cells does not lead to galectin puncta on endosomes. Experiment was repeated 2 times independently with similar results (scale bar: 1 μ m).



Supplementary Figure 4. EGFR Trafficking and DiIC₁₆-SiR imaging with HeLa cells

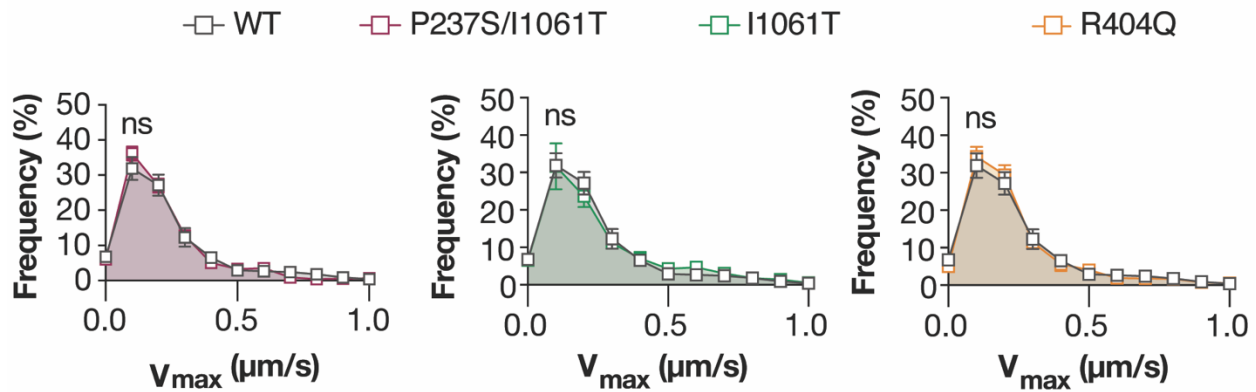
expressing GFP-Rab7. (a) HeLa cells expressing both SNAP-EGFR and GFP-Rab7 were treated with DiIC₁₆TCO or DiIC₁₆TCO, SNAP-Surface-647, and EGF, and visualized over 50 min using spinning disk confocal microscopy. (b) Representative SDCM images of AF647-EGFR and GFP-Rab7-positive HeLa cells with and without 5 μ M DiIC₁₆TCO or DiIC₁₆TCO after stimulation with 100 ng/ μ L. Each frame is a merge of 13 1- μ m stacks through the cell, taken every 10 minutes. Images were processed on Volocity (Perkin Elmer), scale bar: 10 μ m. (c) Representative SDCM images of AF647-EGFR and GFP-Rab7-positive HeLa cells without HIDE probe and EGF. Each frame is a merge of 13 1- μ m stacks through the cell, taken every 10 minutes. Experiment was repeated 2 times independently with similar results, images were processed on Volocity (Perkin Elmer), scale bar: 10 μ m. (d) HeLa cells expressing GFP-Rab7 were labeled with DiIC₁₆-SiR as described in Methods and imaged with laser-scanning confocal microscopy over 24 hours. Experiment was repeated 2 times independently with similar results, scale bar: 10 μ m. (e) The location of DiIC₁₆-SiR remains unchanged with respect to GFP-Rab7 over 24 hours. Colocalization between GFP-Rab7 and DiIC₁₆-SiR was measured using the JaCOP plugin on Fiji, n = 6 biologically independent samples for each time point. centerline and error bars represent average with s.e.m. (****p < 0.0001, ***p < 0.001, **p < 0.01, *p < 0.05, and not significant (ns) for p > 0.05, one-way ANOVA followed by Tukey's multiple comparisons test).



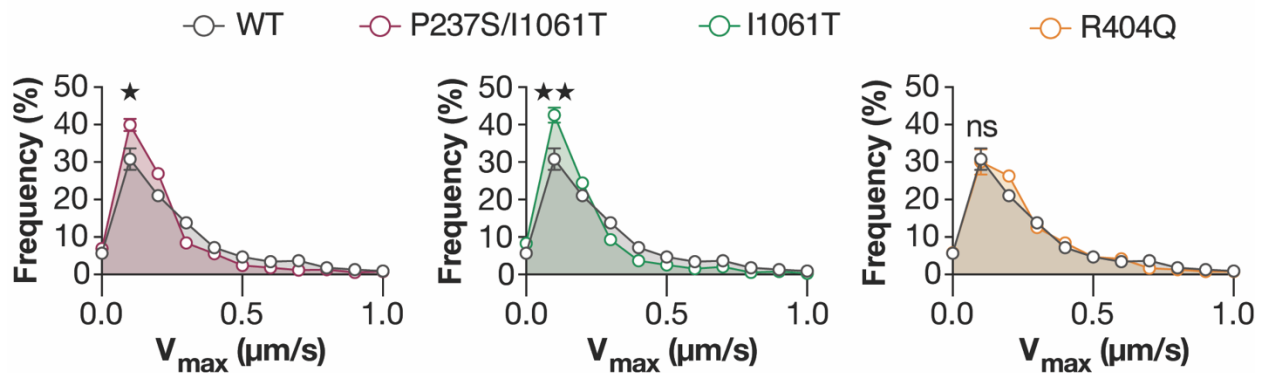
Supplementary Figure 5. Long-term imaging with DiIC₁₆-SiR, DiIC₁₆'-SiR and Rab7-SiR and effects on cell viability (a) HeLa cells labeled with DiIC₁₆(3), DiIC₁₆TCO, or DiIC₁₆'TCO continue to divide for over 20 hours. Cells were labeled and imaged over 20 hours in DMEM (with 10% FBS and 1X pen/strep) at 37°C with 5% CO₂. Experiment was repeated 2 times

independently with similar results, scale bar: 20 μm . (b) One-hour or overnight incubation with DiIC₁₆-SiR does not significantly alter nuclear DNA content. HeLa cells were labeled with DiIC₁₆TCO and SiR-Tz as described in the Methods section and subsequently incubated at 37°C (with 5% CO₂) in DMEM (with 10% FBS and pen/strep) for either 24 hours or 1 hour. Immediately before flow cytometry, the cells were treated with 300 nM Hoescht 33342 for 10 minutes alongside HeLa cells that were not treated with DiIC₁₆TCO and SiR-Tz. The cells were then lifted off the glass dish with Trypsin LE, resuspended in DMEM (with 10% FBS and pen/strep), and centrifuged to remove any cell debris. This pellet was resuspended in DPBS and subsequently analyzed on an Attune NxT flow cytometer. The median fluorescent intensity (MFI) was collected from three distinct samples of HeLa cells for each condition, centerline and error bars represent average with s.e.m. All samples were compared to cells stained with only Hoescht 33342. (****p < 0.0001, ***p < 0.001, **p < 0.01, *p < 0.05, and not significant (ns) for p > 0.05, one-way ANOVA). Experiment was repeated once independently with similar results. (c) SiR photobleaching with DiIC₁₆-SiR, DiIC₁₆'-SiR, and Halo-Rab7 and SiR-CA with STED microscopy. SiR-Rab7 videos were obtained at 1 frame/2s for 30-40 frames total. DiIC₁₆-SiR and DiIC₁₆'-SiR videos were obtained at 1.93 frames/s with bidirectional x-scanning. Experiment was repeated 3 times independently with similar results. Field of view in both cases is 19.38 μm x 19.38 μm , scale bar = 1 μm .

a Confocal



b STED



Supplementary Figure 6: STED and Confocal Tracking of Endosomes in WT Fibroblasts

(a) Endosome motility differences in NPD fibroblasts labeled with DiIC₁₆-SiR when measured with laser-scanning confocal microscopy. Data represents average V_{max} distribution from $n = 4$ biologically independent samples for each mutant, where error bars represent s.e.m. (*** $p < 0.001$, ** $p < 0.01$, * $p < 0.05$, and not significant (ns) for $p > 0.05$, one-way ANOVA comparison followed by Dunnett's multiple comparison test of the median V_{max} values from each mutant fibroblast line to WT fibroblasts). Experiment was repeated once independently with similar results. (b) Endosome motility differences in NPD fibroblasts labeled with DiIC₁₆-SiR when measured with STED microscopy (same data as shown in **Figure 5e** in the main text, shown here for easier comparison). Data represents average V_{max} distribution from $n = 10$ biologically independent samples for each mutant, where error bars represent s.e.m. (*** $p < 0.001$, ** $p < 0.01$, * $p < 0.05$, and not significant (ns) for $p > 0.05$, one-way ANOVA comparison followed by

Dunnett's multiple comparison test of the median V_{\max} values from each mutant fibroblast line to WT fibroblasts).

Legends for Supplementary Videos

Supplementary Video 1: HeLa cells labeled with DiIC₁₆-SiR.

HeLa cells were labeled with DiIC₁₆TCO and SiR-Tz as described in the Methods section. STED microscopy was performed on a Leica TCS SP8 Gated STED 3x microscope equipped with a tunable pulsed white light laser (460 – 660 nm) for excitation and two HyD detectors for tunable spectral detection. For live-cell imaging, the microscope was equipped with a Tokai Hit stage top incubator (model: INUBG2A-GSI) with temperature and CO₂ control to maintain an environment of 37°C and 5% CO₂. In this work, SiR derivatives were excited at 633 nm (15% power) and their emission was detected using a HyD detector from 650-737 nm. The 775 nm depletion laser was used for STED microscopy (20% power). Imaging was conducted with a 100x oil immersion objective (HC PL APO 100x/1.40 Oil) at 1000 Hz with 1-line accumulation and bi-directional x-scanning in a 19.38 μm² field of view (1024 x 1024 pixels at 18.94 nm/pixel). Raw microscopy data were Gaussian blurred (1.0 pixels) in ImageJ. The FWHM value were obtained by fitting line profiles to a Lorentz distribution using Origin 8.2 (www.originlab.com). Experiment was repeated 10 times independently with similar results.

Supplementary Video 2: HeLa cells labeled with DiIC₁₆-SiR.

HeLa cells were labeled with DiIC₁₆TCO and SiR-Tz as described in the Methods section. STED microscopy was performed on a Leica TCS SP8 Gated STED 3x microscope equipped with a tunable pulsed white light laser (460 – 660 nm) for excitation and two HyD detectors for tunable spectral detection. For live-cell imaging, the microscope was equipped with a Tokai Hit stage top incubator (model: INUBG2A-GSI) with temperature and CO₂ control to maintain an environment of 37°C and 5% CO₂. In this work, SiR derivatives were excited at 633 nm (15% power) and their emission was detected using a HyD detector from 650-737 nm. The 775 nm depletion laser was used for STED microscopy (20% power). Imaging was conducted with a 100x oil immersion objective (HC PL APO 100x/1.40 Oil) at 1000 Hz with 1-line accumulation and bi-directional x-scanning in a 19.38 μm² field of view (1024 x 1024 pixels at 18.94 nm/pixel). Raw microscopy data were Gaussian blurred (1.0 pixels) in ImageJ. The FWHM value were obtained by fitting line profiles to a Lorentz distribution using Origin 8.2 (www.originlab.com). Experiment was repeated 5 times independently with similar results.

Supplementary Video 3: WT (GM05399) fibroblasts labeled with DiIC₁₆-SiR.

WT fibroblasts were labeled with DiIC₁₆TCO and SiR-Tz as described in the Methods section for HeLa cells. STED microscopy was performed on the same instrument as described in Supplementary Video 1. For imaging WT Fibroblasts, SiR derivatives were excited at 633 nm (20% power) and their emission was detected using a HyD detector from 650-737 nm. The 775 nm depletion laser was used for STED microscopy (20% power). For simultaneous STED and confocal microscopy, cells were imaged with sequential excitation with 561 nm (for DiI) and 633 nm with 775 nm depletion (for SiR), enabling confocal/STED microscopy of the same cell with a frame rate of 5.814 s/frame. Imaging was conducted at 1000 Hz with 1-line accumulation and bi-directional x-scanning in a 19.38 μm² field of view (1024 x 1024 pixels at 18.94 nm/pixel) for single-color STED microscopy, or with a 9.69 μm² field of view (512 x 512 pixels at 18.96 nm/pixel) for simultaneous confocal/STED imaging (Figure 4e and 5a). Raw microscopy data

from STED imaging were Gaussian blurred (1.0 pixels) in ImageJ. Experiment was repeated 6 times independently with similar results.

Supplementary Video 4: I1061T (GM18453) Fibroblasts labeled with DiIC₁₆-SiR

Homozygous I1061T fibroblasts were labeled with DiIC₁₆TCO and SiR-Tz as described in the Methods section for HeLa cells. STED microscopy was performed on the same instrument as described in Supplementary Movie 1. For imaging I1061T Fibroblasts, SiR derivatives were excited at 633 nm (20% power) and their emission was detected using a HyD detector from 650-737 nm. The 775 nm depletion laser was used for STED microscopy (20% power). Imaging was conducted at 1000 Hz with 1-line accumulation and bi-directional x-scanning in a 19.38 μm^2 field of view (1024 x 1024 pixels at 18.94 nm/pixel) for single-color STED microscopy. Raw microscopy data from STED imaging were Gaussian blurred (1.0 pixels) in ImageJ. Experiment was repeated 5 times independently with similar results.

Supplementary Video 5: P237S/I1061T (GM03123) Fibroblasts labeled with DiIC₁₆-SiR

Heterozygous I1061T/P237S fibroblasts were labeled with DiIC₁₆TCO and SiR-Tz as described in the Methods section for HeLa cells. STED microscopy was performed on the same instrument as described in Supplementary Movie 1. For imaging I1061T/P237S Fibroblasts, SiR derivatives were excited at 633 nm (20% power) and their emission was detected using a HyD detector from 650-737 nm. The 775 nm depletion laser was used for STED microscopy (20% power). Imaging was conducted at 1000 Hz with 1-line accumulation and bi-directional x-scanning in a 19.38 μm^2 field of view (1024 x 1024 pixels at 18.94 nm/pixel) for single-color STED microscopy. Raw microscopy data from STED imaging were Gaussian blurred (1.0 pixels) in ImageJ. Experiment was repeated 5 times independently with similar results.

Supplementary Video 6: R404Q (GM18388) Fibroblasts labeled with DiIC₁₆-SiR

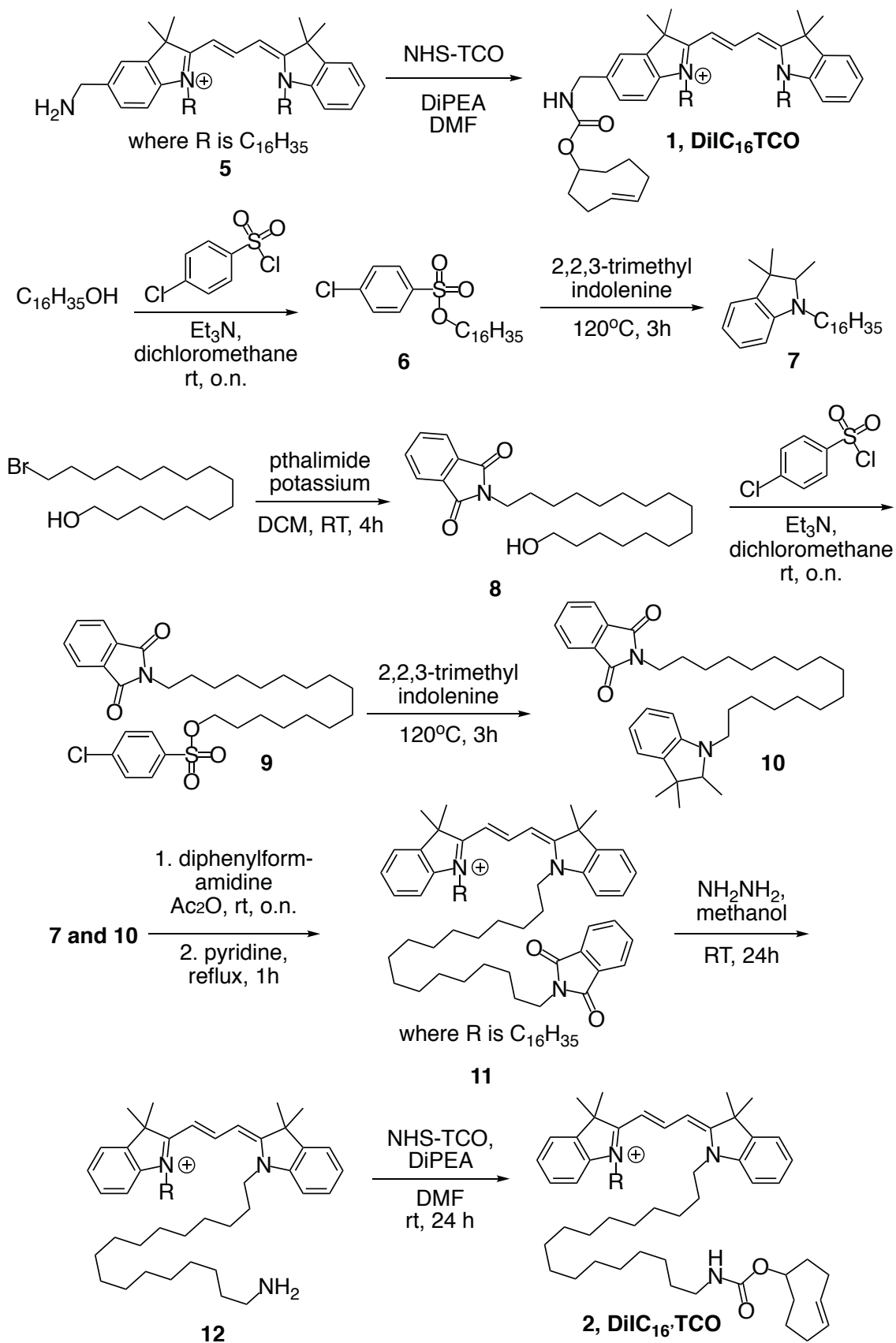
Homozygous R404Q fibroblasts were labeled with DiIC₁₆TCO and SiR-Tz as described in the Methods section for HeLa cells. STED microscopy was performed on the same instrument as described in Supplementary Movie 1. For imaging R404Q Fibroblasts, SiR derivatives were excited at 633 nm (20% power) and their emission was detected using a HyD detector from 650-737 nm. The 775 nm depletion laser was used for STED microscopy (30% power). Imaging was conducted at 1000 Hz with 1-line accumulation and bi-directional x-scanning in a 19.38 μm^2 field of view (1024 x 1024 pixels at 18.94 nm/pixel) for single-color STED microscopy. Raw microscopy data from STED imaging were Gaussian blurred (1.0 pixels) in ImageJ. Experiment was repeated 5 times independently with similar results.

Supplementary Video 7: 1920delG (GM23945) Fibroblasts labeled with DiIC₁₆-SiR

1920delG fibroblasts were labeled with DiIC₁₆TCO and SiR-Tz as described in the Methods section for HeLa cells. STED microscopy was performed on the same instrument as described in Supplementary Movie 1. For imaging 1920delG fibroblasts, SiR derivatives were excited at 633 nm (20% power) and their emission was detected using a HyD detector from 650-737 nm. The 775 nm depletion laser was used for STED microscopy (20% power). Imaging was conducted at 1000 Hz with 1-line accumulation and bi-directional x-scanning in a 19.38 μm^2 field of view (1024 x 1024 pixels at 18.94 nm/pixel) for single-color STED microscopy. Raw

microscopy data from STED imaging were Gaussian blurred (1.0 pixels) in ImageJ. Experiment was repeated 5 times independently with similar results.

Supplementary Note: Synthesis of DiIC₁₆TCO and DiIC_{16'}TCO



Materials, reagents, and instrumentation for chemical synthesis

Chemicals used for synthesis, purchased from Wako Pure Chemical, Thermo Fisher Scientific, Kerfast, Tokyo and Aldrich Chemical Company, were of the highest grade available and were used without further purification. All solvents were purchased as reagent grade from Aldrich without purification. Flash chromatography was performed using a Teledyne Isco CombiFlash Rf using pre-packed columns with RediSep Rf silica (40–60 μm). ^1H NMR and ^{13}C NMR spectra were recorded on a Bruker AVANCEIII 400 (400 MHz for ^1H and 101 MHz for ^{13}C) or an Agilent DD2 600 NMR spectrometer (600 MHz for ^1H and 151 MHz for ^{13}C). The values of chemical shifts (δ) are reported in p.p.m. relative to the solvent residual signals of CD_3OD (3.31 p.p.m. for ^1H , 49.00 p.p.m. for ^{13}C), CD_2Cl_2 (5.33 p.p.m. for ^1H , 53.84 p.p.m. for ^{13}C) or CDCl_3 (7.26 p.p.m. for ^1H , 77.36 p.p.m. for ^{13}C). High-resolution mass spectra (HRMS) were recorded on a **Bruker micrOTOFII** with electron spray ionization (ESI).

Synthesis of $\text{DiIC}_{16}\text{TCO}$ (1)

5-((((((E)-cyclooct-4-en-1-yl)oxy)carbonyl)amino)methyl)-1-heptadecyl-2-((E)-3-((Z)-1-heptadecyl-3,3-dimethylindolin-2-ylidene)prop-1-en-1-yl)-3,3-dimethyl-3H-indol-1-ium ($\text{DiIC}_{16}\text{TCO}$, 1)

5 (16 mg, 0.0198 mmol) was synthesized as previously reported (Leung, W. Y.; Haugland, R. P.; Mao, F US6004536A. **1999**) and was dissolved in dimethylformamide (2 mL) in a scintillation vial equipped with magnetic stir bar under argon. Diisopropylethyl amine (0.2 mL, 1.194 mmol) was added to the stirring mixture, followed by the N-hydroxysuccinimide trans-cyclooctene (Kerfast, 13 mg, 0.0486 mmol). The reaction mixture was then stirred overnight at room temperature. This mixture was then concentrated under vacuum and then extracted between diethyl ether and brine three times. The organic layers were combined, dried over Na_2SO_4 , filtered and concentrated. The resulting residue was purified by silica flash chromatography with 25% methanol in 1:1 ethyl acetate:chloroform as the eluent at 98% purity.

^1H NMR (CDCl_3 , 500 MHz): δ (p.p.m.) = 8.83 (t, 1H), 7.37 (m, 5H), 7.04-7.12 (dd, 2H), 6.95 – 7.19 (m, 2H), 5.55 (m, 2H), 4.39 (bt, 2H), 4.21 (bt, 4H), 3.64 (s, 1H), 2.35 (m, 2H), 2.04 (m, 1H) 1.92 (m, H), 1.84 (m, 2H), 1.71 (d, 12H), 1.48 (m, 4H), 1.25 (s, 44H), 0.87 (t, 6H).

^{13}C NMR (CDCl_3 , 151 MHz): δ (p.p.m.) = 173.53, 150.58, 142.29, 141.57, 141.10, 140.61, 134.92, 132.93, 128.77, 127.89, 127.74, 125.13, 122.06, 110.93, 80.92, 77.20, 76.99, 76.78,

70.55, 48.92, 41.13, 38.65, 34.26, 32.51, 31.90, 30.96, 29.68, 29.64, 29.62, 29.50, 29.47, 29.45, 29.34, 28.15, 28.12, 27.69, 27.66, 26.89, 22.67, 14.11.

HRMS (ESI+) (m/z): [M] calculated for $C_{65}H_{104}N_3O_2^+$ = 959.57, found 959.79 [M].

Synthesis of DiIC₁₆TCO (2)

2-(16-hydroxyhexadecyl)isoindoline-1,3-dione (8)

16-bromohexadecanol (100 mg, 1.556 mmol) and potassium phthalimide (56 mg, 1.556 mmol) were dissolved in anhydrous dimethylformamide in a 100 mL round bottom flask equipped with magnetic stir bar under argon, and the reaction was stirred at room temperature overnight. The reaction mixture was diluted with diethyl ether and extracted with NaHCO₃, water, and brine. The aqueous layers were combined and rinsed with diethyl ether. The organic layers were combined, dried over Na₂SO₄, and concentrated to afford the product **8** in quantitative yield with sufficient purity (> 95%).

¹H NMR (CD₃OD, 500 MHz): δ (p.p.m.) = 7.81 (m, 4H), 4.87 (s, H₂O), 3.54 (t, 2H), 3.42 (t, 2H), 1.83 (p, 2H), 1.52 (p, 2H), 1.43 (p, 2H), 1.28 (s, 22H).

¹³C NMR (101 MHz, CD₃OD) δ (p.p.m.) = 170.81, 135.26, 134.23, 124.05, 79.48, 79.14, 78.82, 62.98, 49.65, 49.45, 49.42, 49.24, 49.21, 49.02, 49.00, 48.81, 48.79, 48.60, 48.58, 48.37, 34.33, 33.95, 33.60, 30.70, 30.67, 30.66, 30.59, 30.55, 30.52, 29.80, 29.13, 26.89.

HRMS (ESI+) (m/z): [M] calculated for C₂₄H₃₇NO₃ = 387.28, found 388.27 [M + H].

16-(1,3-dioxoisoindolin-2-yl)hexadecyl 4-chlorobenzenesulfonate (9)

8 (120 mg, 0.310 mmol) and para-chlorobenzene sulfonylchloride (66 mg, 0.310 mmol) were dissolved in anhydrous dichloromethane in a 100 mL round bottom flask equipped with magnetic stir bar under argon. Triethylamine (0.084 mL, 0.620 mmol) was added dropwise and the reaction was stirred at room temperature overnight. The reaction mixture was then extracted water three times. The aqueous layers were combined and rinsed with dichloromethane. The organic layers were combined, dried over Na₂SO₄, and concentrated to afford the product **9** in quantitative yield with sufficient purity (> 98%).

¹H NMR (CDCl₃, 500 MHz): δ (p.p.m.) = 7.84 (m, 4H), 7.71 (m, 2H), 7.53 (d, 2H), 4.05 (t, 2H), 3.67 (t, 2H), 3.60 (m 1.65 (m, 4H), 1.32 (s, 6H), 1.24 (s, 20H), 0.8 (m, hexanes).

^{13}C NMR (151 MHz, CDCl_3) δ (p.p.m.) = 174.27, 169.34, 168.84, 142.19, 140.13, 139.63, 136.84, 134.22, 133.83, 133.78, 132.57, 131.05, 130.31, 129.32, 128.93, 128.74, 128.29, 128.02, 127.97, 127.91, 127.06, 122.86, 77.48, 77.16, 76.84, 71.12, 65.21, 61.88, 48.89, 48.69, 48.48, 48.27, 48.05, 47.84, 47.62, 45.92, 37.68, 33.51, 32.47, 32.14, 29.27, 29.22, 29.19, 29.15, 29.11, 29.09, 29.06, 28.99, 28.95, 28.78, 28.49, 28.37, 28.18, 28.01, 27.76, 26.47, 25.52, 25.43, 24.90.

HRMS (ESI+) (m/z): [M] calculated for $\text{C}_{30}\text{H}_{40}\text{ClNO}_5\text{S}$ = 561.23, found 562.34 [M + H].

2-(16-(2,3,3-trimethylindolin-1-yl)hexadecyl)isoindoline-1,3-dione (10)

9 (160 mg, 0.285 mmol) and 2,3,3-trimethylindolenine (0.05 mL, 0.285 mmol) were combined together in a 100 mL round bottom flask and stirred for 3 hours at 120°C . The reaction mixture was cooled to room temperature and extracted between ethyl acetate and water. The organic layers were combined, dried over Na_2SO_4 , filtered and concentrated to give the title compound as the major product (70% purity, used in the synthesis of **11** without further purification).

^1H NMR (CDCl_3 , 600 MHz): δ (p.p.m.) = 7.87 (m, 2H), 7.76 (m, 2H), 3.46 (t, 2H), 3.40 (t, 2H), 1.85 (m, 2H), 1.60 (s, 3H), 1.32 (s, 6H), 1.26 (s, 28H).

^{13}C NMR (101 MHz, CDCl_3) δ (p.p.m.) = 168.35, 134.34, 133.95, 132.78, 131.37, 130.01, 129.20, 128.99, 128.51, 128.02, 123.63, 123.25, 121.95, 77.48, 77.16, 76.84, 71.07, 65.94, 63.13, 45.31, 34.18, 32.94, 32.87, 29.79, 29.74, 29.66, 29.55, 29.45, 29.00, 28.88, 28.50, 28.28, 27.28, 26.99, 26.31, 26.05, 25.85, 24.54, 24.40..

HRMS (ESI+) (m/z): [M] calculated for $\text{C}_{35}\text{H}_{50}\text{N}_2\text{O}_2^+$ = 530.39, found 530.38 [M].

hexadecyl 4-chlorobenzenesulfonate (6)

Hexadecanol (1g, 4.125 mmol) and para-chlorobenzene sulfonylchloride (871 mg, 4.125 mmol) were dissolved in anhydrous dichloromethane in a 100 mL round bottom flask equipped with magnetic stir bar under argon. Triethylamine (1.2 mL, 8.249 mmol) was added dropwise and the reaction was stirred at room temperature overnight. The reaction mixture was then extracted water three times. The aqueous layers were combined and rinsed with dichloromethane. The organic layers were combined, dried over Na_2SO_4 , and concentrated to afford the product **1** in quantitative yield with >99% purity, as previously reported.

^1H NMR (CDCl_3 , 500 MHz): δ (p.p.m.) = 7.84 (d, 2H), 7.53 (d, 2H), 4.05 (t, 2H), 1.64 (p, 2H), 1.25 (s, 20H), 0.86 (t, 3H).

HRMS (ESI+) (m/z): [M] calculated for $\text{C}_{22}\text{H}_{37}\text{ClO}_3\text{S}$ = 416.22, found 417.54 [M+H].

1-hexadecyl-2,3,3-trimethyl-3H-indol-1-ium (7)

1 (500 mg, 1.201 mmol) and 2,3,3 – trimethylindolenine (0.2 mL, 1.201 mmol) were combined together in a 100 mL round bottom flask and stirred for 3 hours at 120°C. The reaction mixture was cooled to room temperature and extracted between ethyl acetate and water. The organic layers were dried over Na_2SO_4 , filtered and concentrated to afford product **4** as a deep magenta crystal in sufficient purity (75%), as previously reported.

^1H NMR (CDCl_3 , 500 MHz): δ (p.p.m.) = 7.73 (d, 2H), 7.25 (2H), 4.68 (t, 2H), 3.38 (t, 2H), 2.97 (s, 3H), 1.59 (s, 6H), 1.25 (s, 26H), 0.87 (t, 3H).

HRMS (ESI+) (m/z): [M] calculated for $\text{C}_{27}\text{H}_{46}\text{N}$ = 384.36, found 384.36 [M].

2-((E)-3-((Z)-1-(16-(1,3-dioxoisindolin-2-yl)hexadecyl)-3,3-dimethylindolin-2-ylidene)prop-1-en-1-yl)-1-hexadecyl-3,3-dimethyl-3H-indol-1-ium (11)

7 (150 mg, 0.283 mmol) was added to a 100 mL round bottom flask with diphenylformamidine (61 mg, 0.312 mmol) in acetic anhydride (0.94 mL) under argon. This mixture was sonicated for 10 minutes and then stirred at room temperature overnight. The acetic anhydride was removed under vacuum and **10** (109 mg, 0.283 mmol) was added to the residue. This mixture was refluxed in pyridine (1.3 mL) for 1 hour and subsequently allowed to come to room temperature. Upon cooling, the reaction mixture was extracted between diethyl ether and brine three times, dried over Na_2SO_4 , filtered and concentrated. This residue was run through a silica plug of 5% methanol in 1:1 chloroform: ethyl acetate. All pink fractions were combined to yield a mixture of the un-functionalized and phthalimide-protected compound (NMR not characterized due to known mixture) and used in the next step (70% desired product).

HRMS (ESI+) (m/z): [M] calculated for $\text{C}_{63}\text{H}_{92}\text{N}_3\text{O}_2^+$ (DiIC₁₆-pth) = 923.45 and $\text{C}_{55}\text{H}_{89}\text{N}_2^+$ (DiIC₁₆) = 778.33, found 922.67 [M_{C₁₆-pth}] and 777.66 [M_{C₁₆}].

2-((E)-3-((Z)-1-(16-aminohexadecyl)-3,3-dimethylindolin-2-ylidene)prop-1-en-1-yl)-1-hexadecyl-3,3-dimethyl-3H-indol-1-ium (12)

11 (20 mg, 0.0217 mmol) was dissolved in methanol (1 mL) in a scintillation vial with a magnetic stir bar. Hydrazine hydrate (0.03 mL, 0.650 mmol) was added and the reaction was stirred for 24 hours at room temperature. The reaction mixture was concentrated and the residue was purified by flash chromatography with 25% methanol in chloroform as the eluent. The title compound was obtained at 95% purity.

¹H NMR (CDCl₃, 600 MHz): δ (p.p.m.) = 8.40 (t, 1H), 7.88 (s, 1H), 7.84 (d, 7.84), 7.38 (m, 4H), 7.26 (m, 4H), 6.7 (m, impurity), 4.17 (bs, 4H), 3.68 (t, 2H), 3.4 (m, impurity), 2.94 (bs, 2H), 1.83 (bs, 4H), 1.71 (s, 12H), 1.36 (s, 2H), 1.35 (s, 2H), 1.24 (s, 30H), 1.22 (s, 26H), 0.86 (t, 3H).

¹³C NMR (151 MHz, CDCl₃) δ (p.p.m.) = 181.38, 174.07, 173.92, 150.58, 142.29, 142.24, 140.69, 140.65, 135.49, 129.09, 128.27, 128.24, 127.91, 127.70, 127.67, 126.20, 125.64, 122.51, 122.32, 122.29, 114.05, 111.47, 111.29, 108.50, 108.46, 103.88, 103.71, 77.37, 77.16, 76.95, 49.31, 49.27, 45.00, 44.20, 40.23, 39.97, 39.95, 32.06, 31.15, 29.84, 29.79, 29.70, 29.67, 29.64, 29.63, 29.50, 29.48, 29.43, 29.42, 29.34, 29.31, 29.27, 29.22, 28.96, 28.30, 28.28, 27.82, 27.77, 27.63, 27.52, 27.05, 27.03, 26.98, 26.97, 26.80, 26.66, 24.58, 24.48, 22.83, 14.27.

HRMS (ESI+) (m/z): [M] calculated for C₅₅H₉₀N₃⁺ = 793.35, found 792.75 [M].

2-((E)-3-((Z)-1-(16-((((E)-cyclooct-4-en-1-yl)oxy)carbonyl)amino)hexadecyl)-3,3-dimethylindolin-2-ylidene)prop-1-en-1-yl)-1-hexadecyl-3,3-dimethyl-3H-indol-1-ium (DiIC₁₆TCO, **2)**

12 (5 mg, 0.0063 mmol) was dissolved in dimethylformamide (1 mL) in a scintillation vial equipped with magnetic stir bar under argon. Diisopropylethyl amine (0.003 mL, 0.0189 mmol) was added to the stirring mixture, followed by N-hydroxysuccinimide trans-cyclooctene (Kerafast, 2 mg, 0.0063 mmol). The reaction mixture was then stirred overnight at room temperature. This mixture was then concentrated under vacuum and then extracted between diethyl ether and brine three times. The organic layers were combined, dried over Na₂SO₄, filtered and concentrated. The resulting residue was purified by flash chromatography with 25% methanol in 1:1 ethyl acetate:chloroform as the eluent. The final compound was obtained with 98% purity.

¹H NMR (CDCl₃, 600 MHz): δ (p.p.m.) = 8.40 (t, 1H), 7.38 (m, 4H), 7.25 (t, 2H), 7.12 (d, 2H), 6.87 (d, 1H), 6.81 (d, 1H), 5.50 (m, 2H), 5.3 (m, DCM), 4.17 (s, 4H), 3.65 (s, 1H), 3.60 (m,

impurity), 3.45 (m, diethyl ether), 3.13 (m, 2H), 2.35 (m, 4H), 2.00 (m, 4H), 1.92 (s, 4H), 1.84 (bs, 4H), 1.71 (s, 12H), 1.47 (s, 6H), 1.25 (s, 33H), 1.23 (s, 30H), 0.87 (m, 3H).

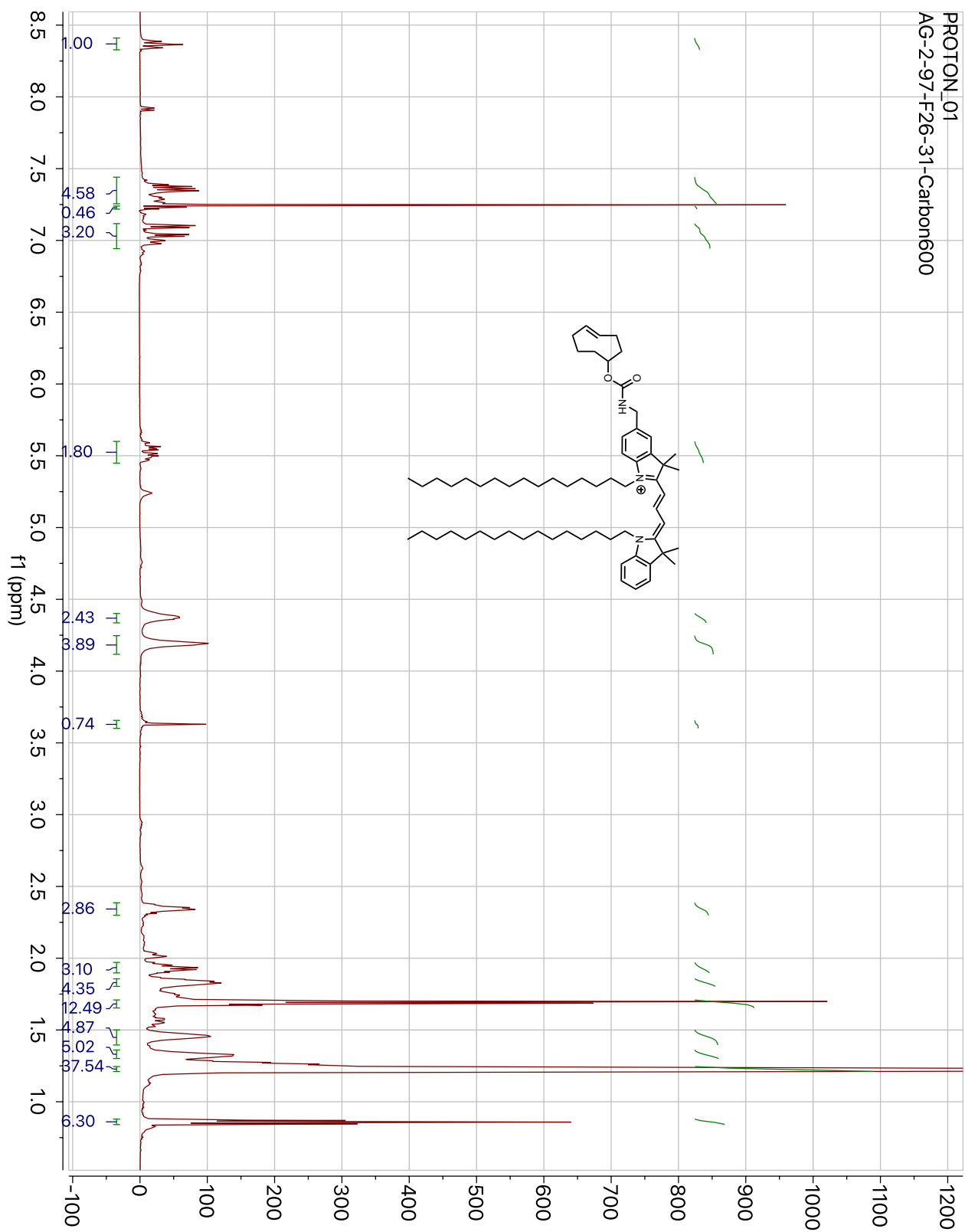
^{13}C NMR (151 MHz, CDCl_3) δ (p.p.m.) = 173.67, 173.65, 150.67, 142.28, 140.61, 134.83, 132.89, 128.78, 127.76, 125.16, 122.02, 113.87, 111.02, 104.36, 77.07, 48.95, 44.76, 41.15, 40.95, 38.66, 34.29, 33.48, 32.51, 31.90, 30.99, 30.92, 30.02, 29.68, 29.66, 29.64, 29.62, 29.58, 29.56, 29.52, 29.46, 29.34, 29.30, 29.26, 28.12, 27.63, 26.85, 26.75, 24.78, 22.67, 14.11, 1.00.

HRMS (ESI+) (m/z): [M] calculated for $\text{C}_{64}\text{H}_{102}\text{N}_3\text{O}_2^+$ ($\text{DiIC}_{16}\text{TCO}$) = 945.54, found 944.81.

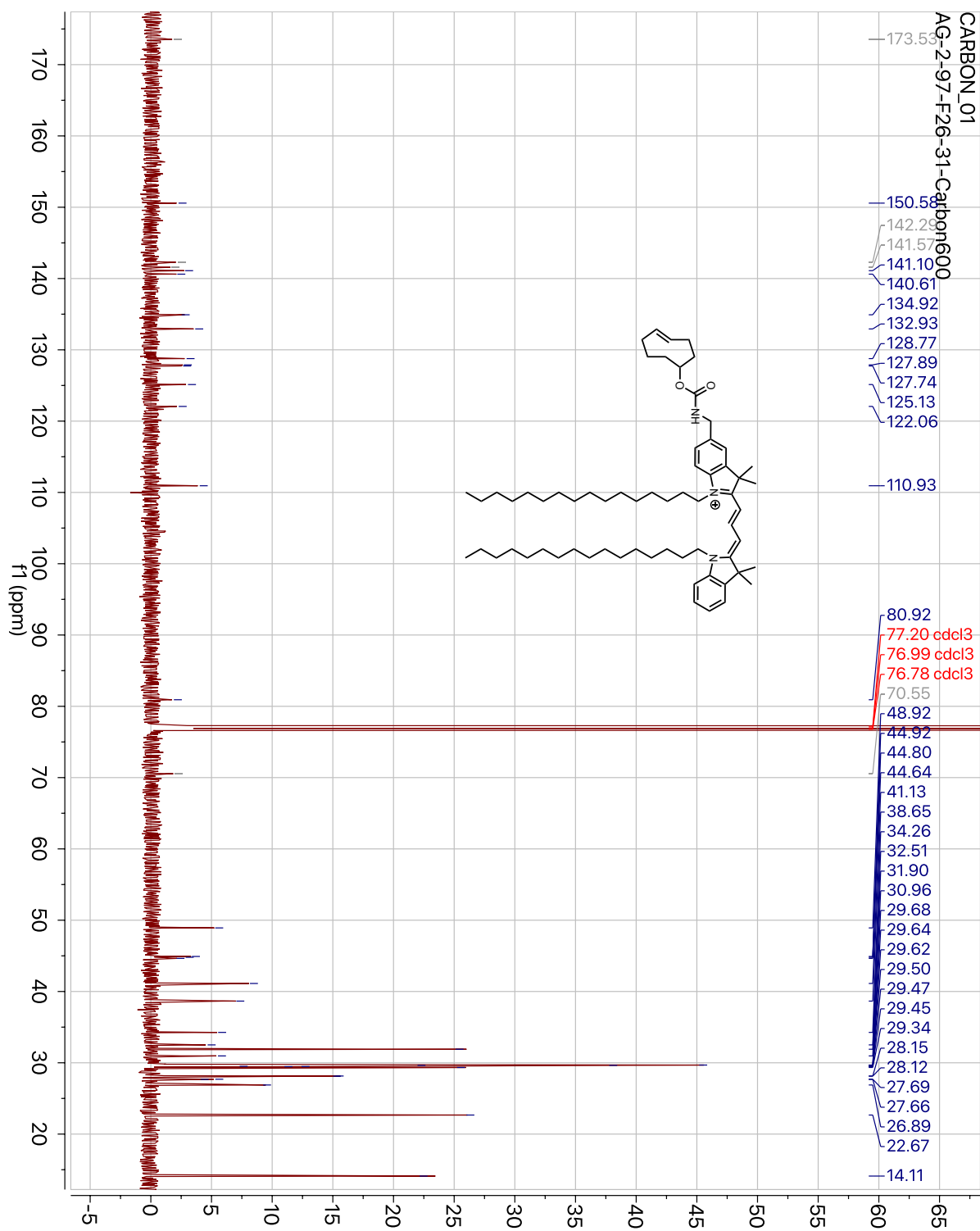
1,1'-Dihexadecyl-3,3',3'-Tetramethylindocarbocyanine Perchlorate ($\text{DiIC}_{16}(3)$, 4)

$\text{DiIC}_{16}(3)$ was purchased from Life Technologies at the highest purity available and used without further purification.

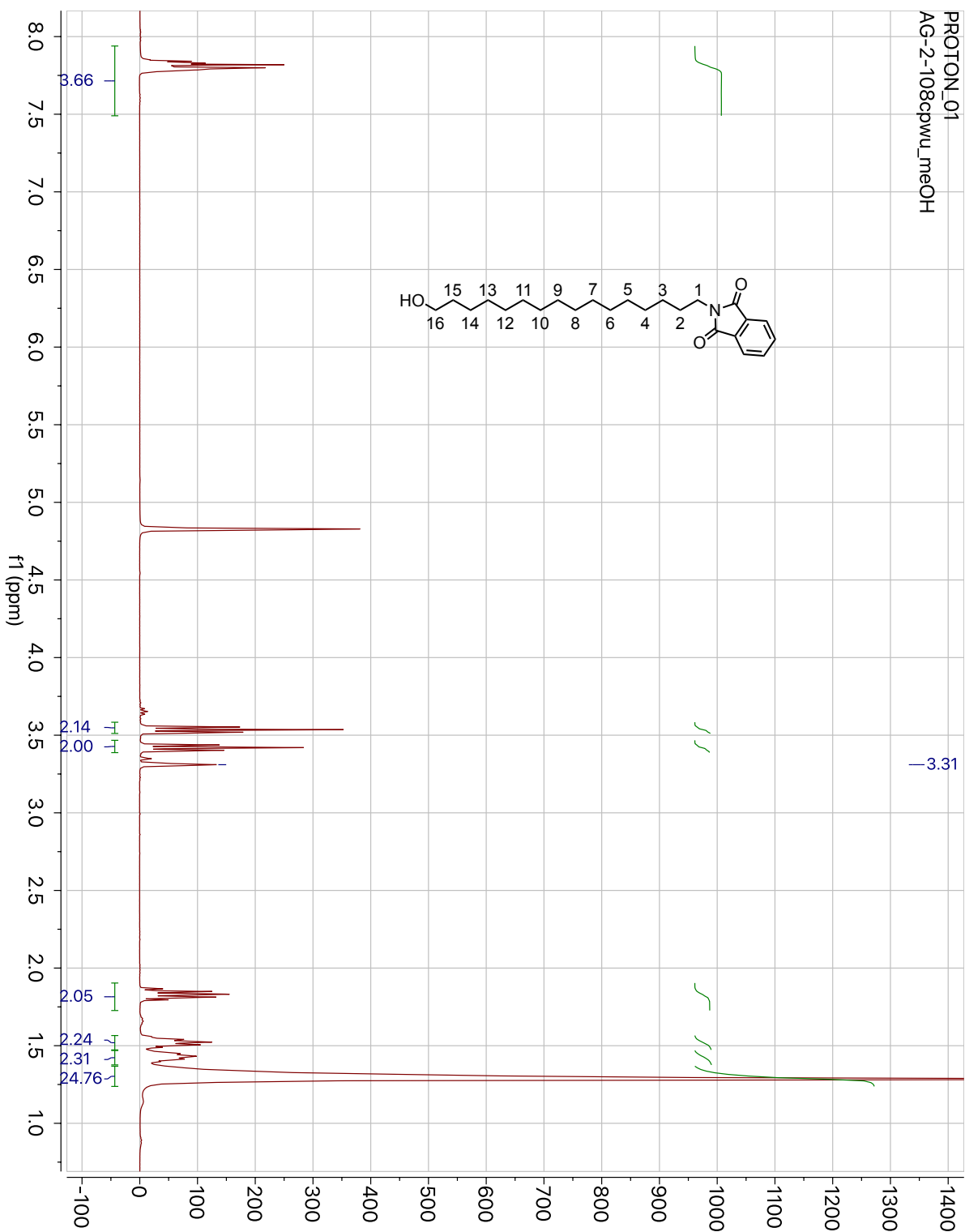
^1H NMR: DiIC₁₆TCO (1)



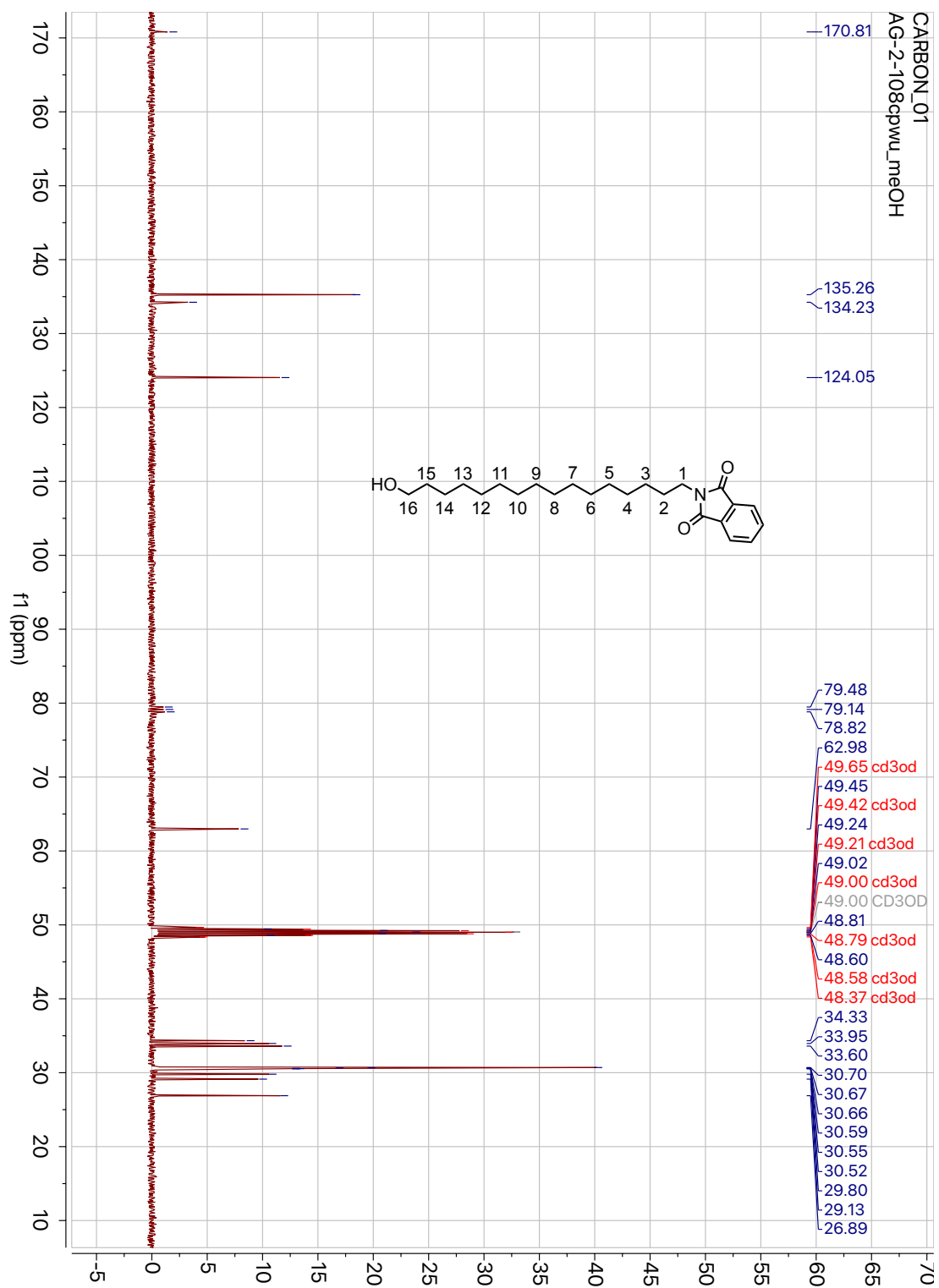
¹³C NMR: DiIC₁₆TCO (1)



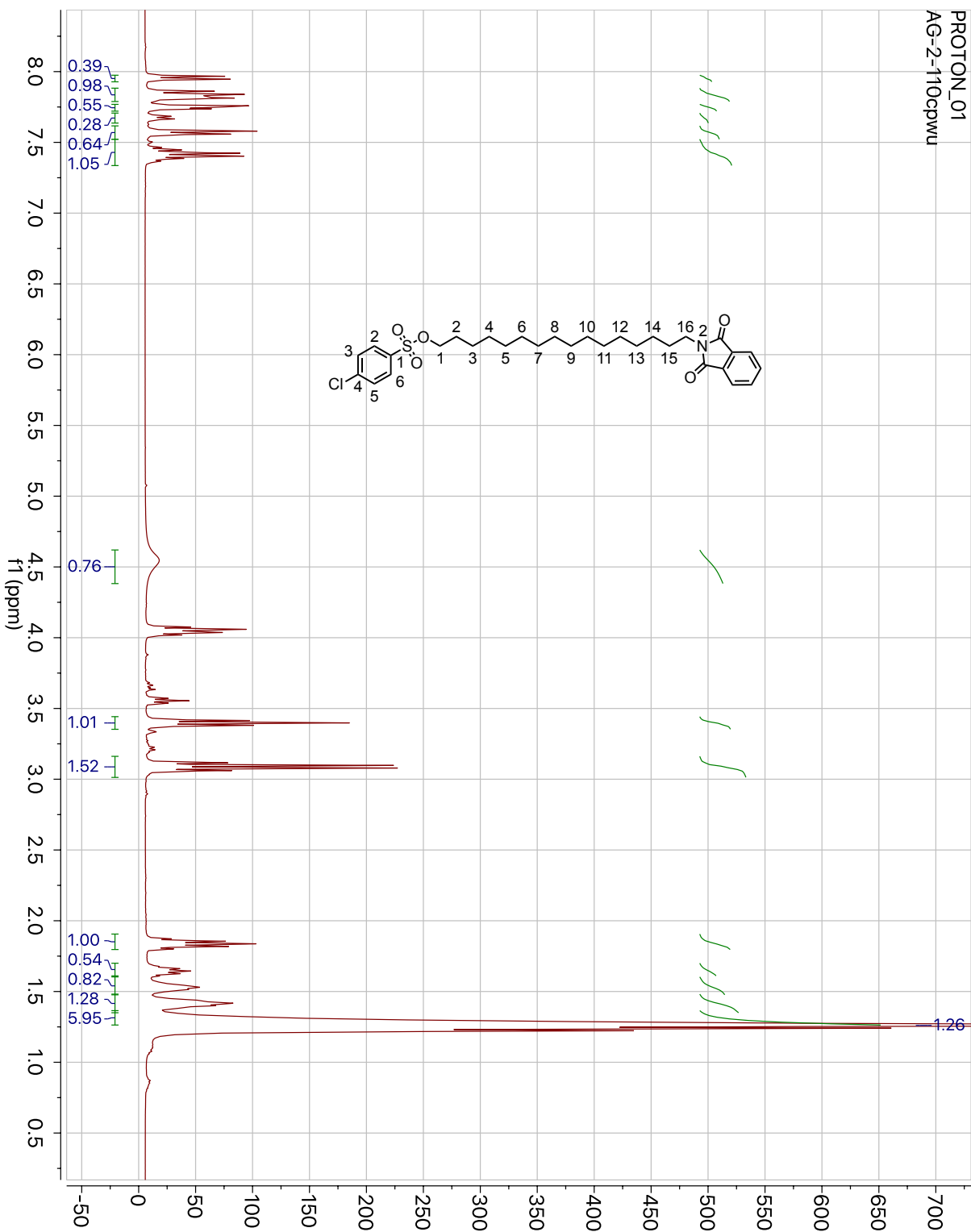
Compound 8: ¹H NMR



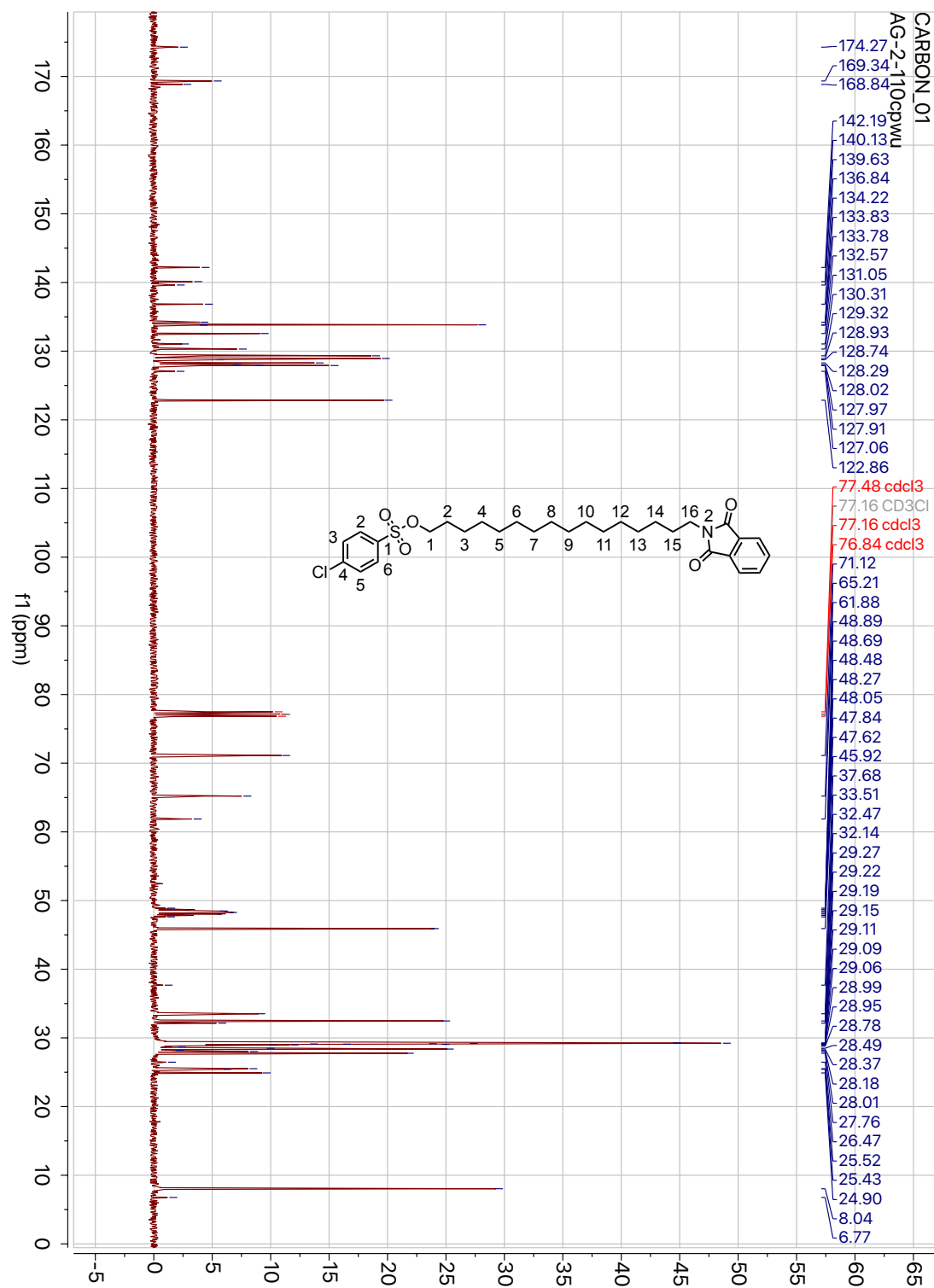
Compound 8: ^{13}C NMR



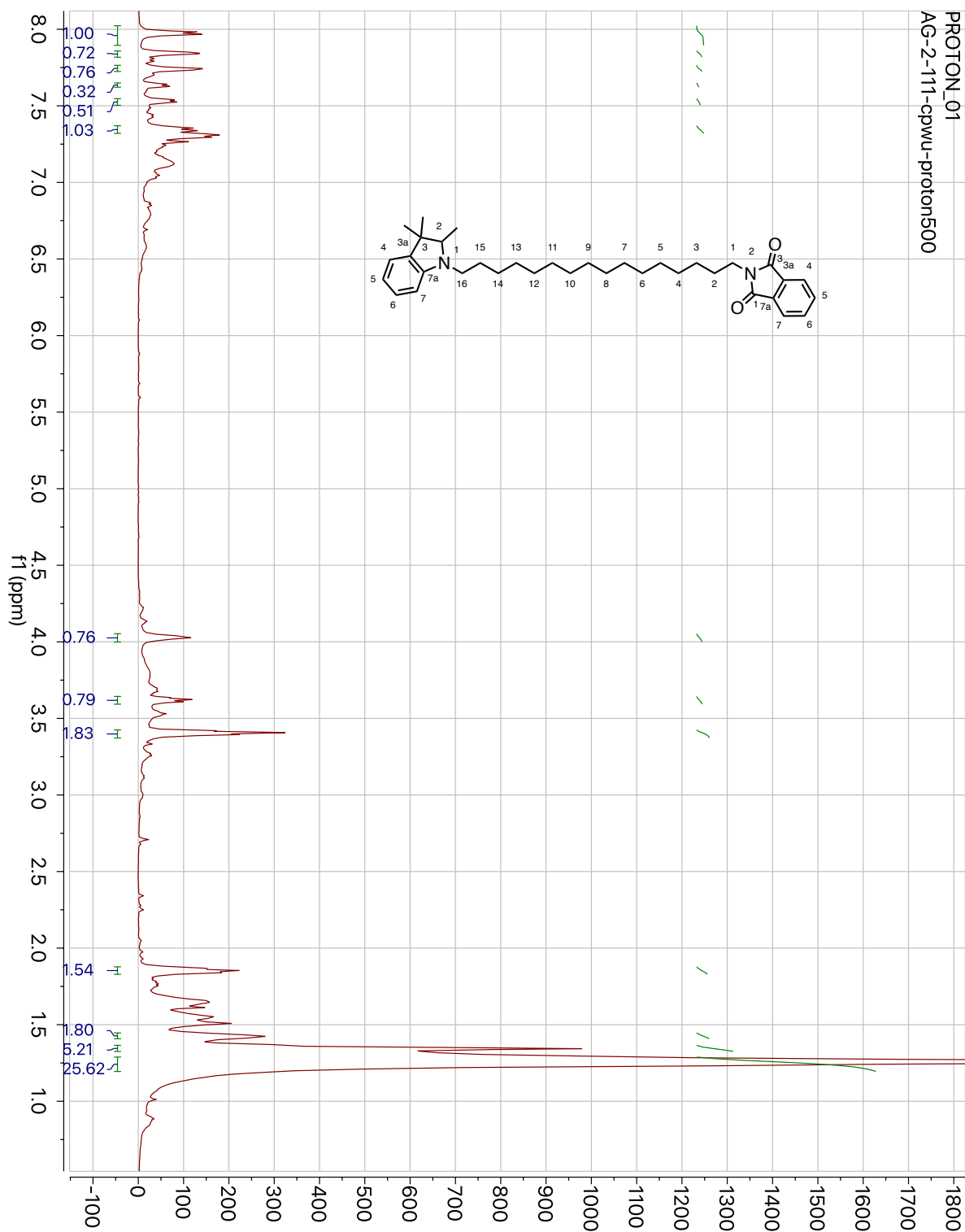
Compound 9: H¹ NMR



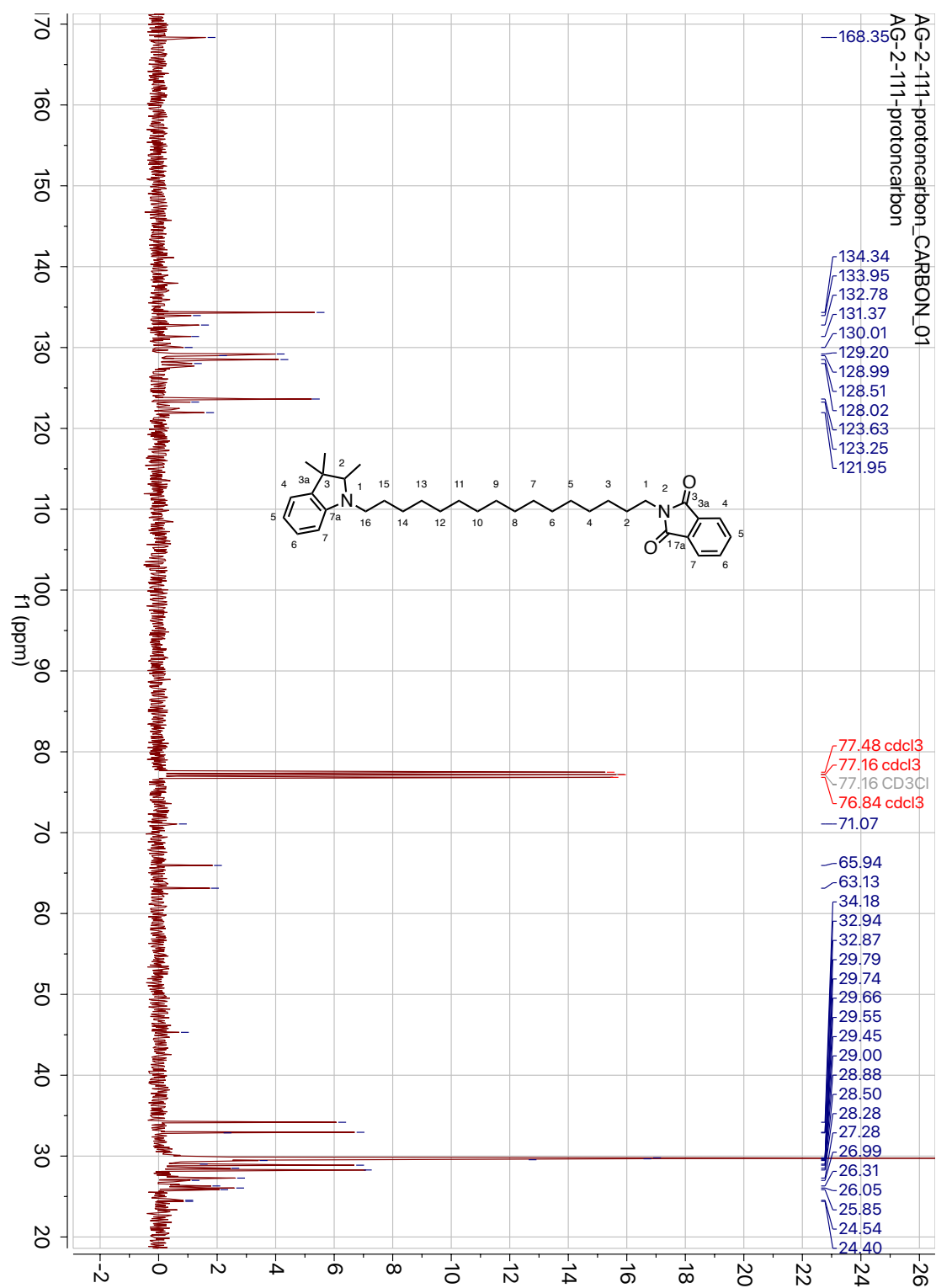
Compound 9: ^{13}C NMR



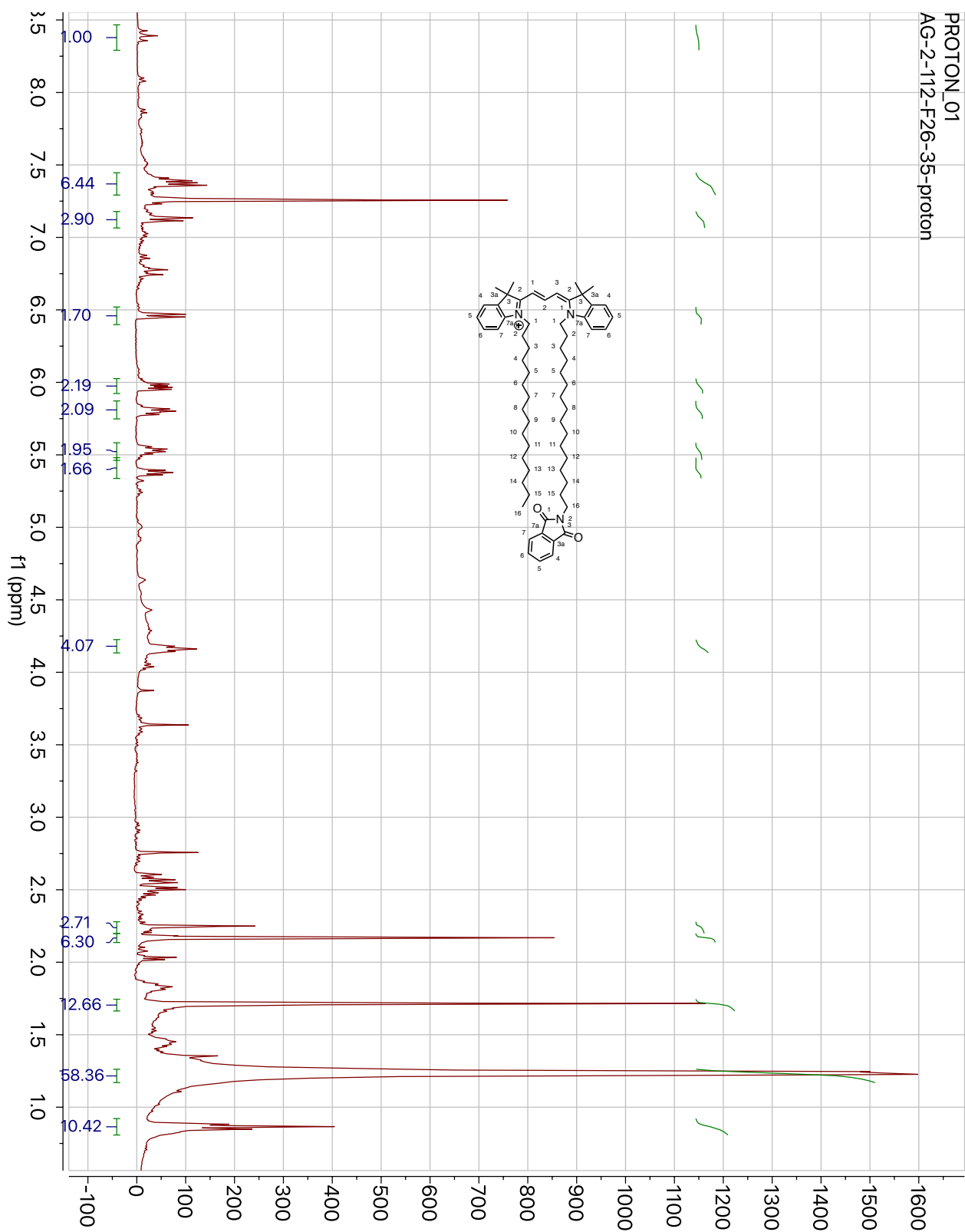
Compound 10: H¹ NMR



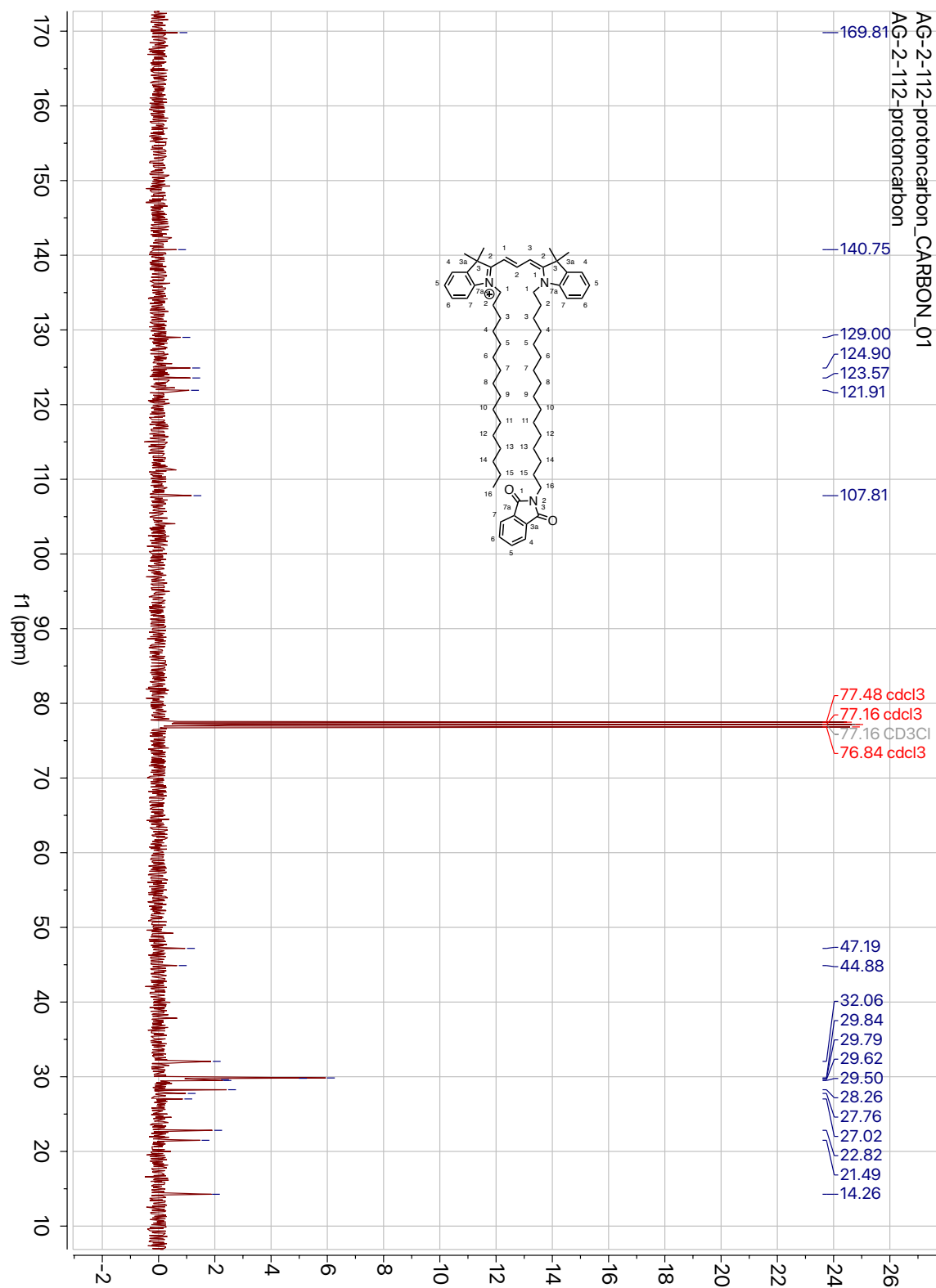
Compound 10: ¹³C NMR



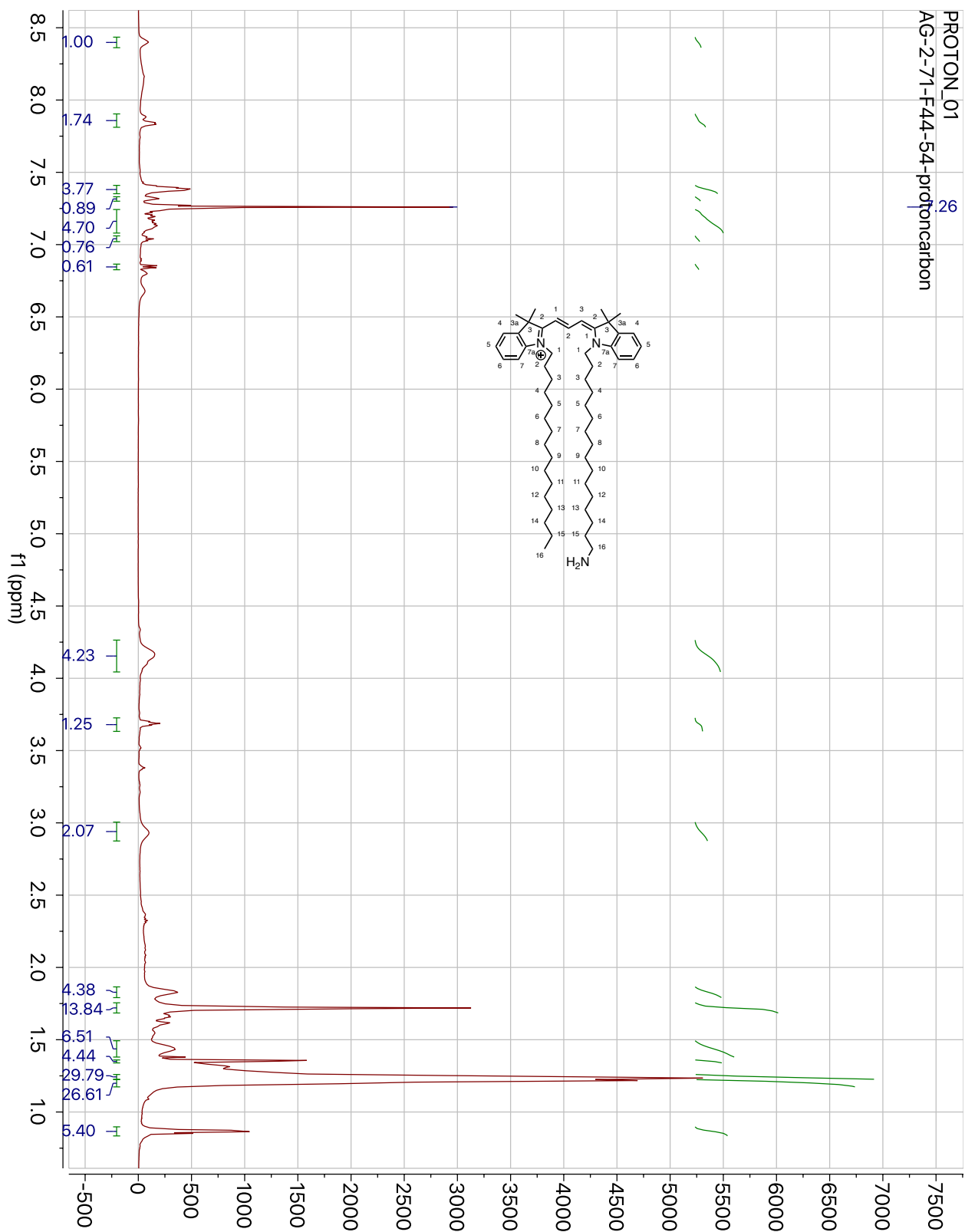
Compound 11: H¹ NMR



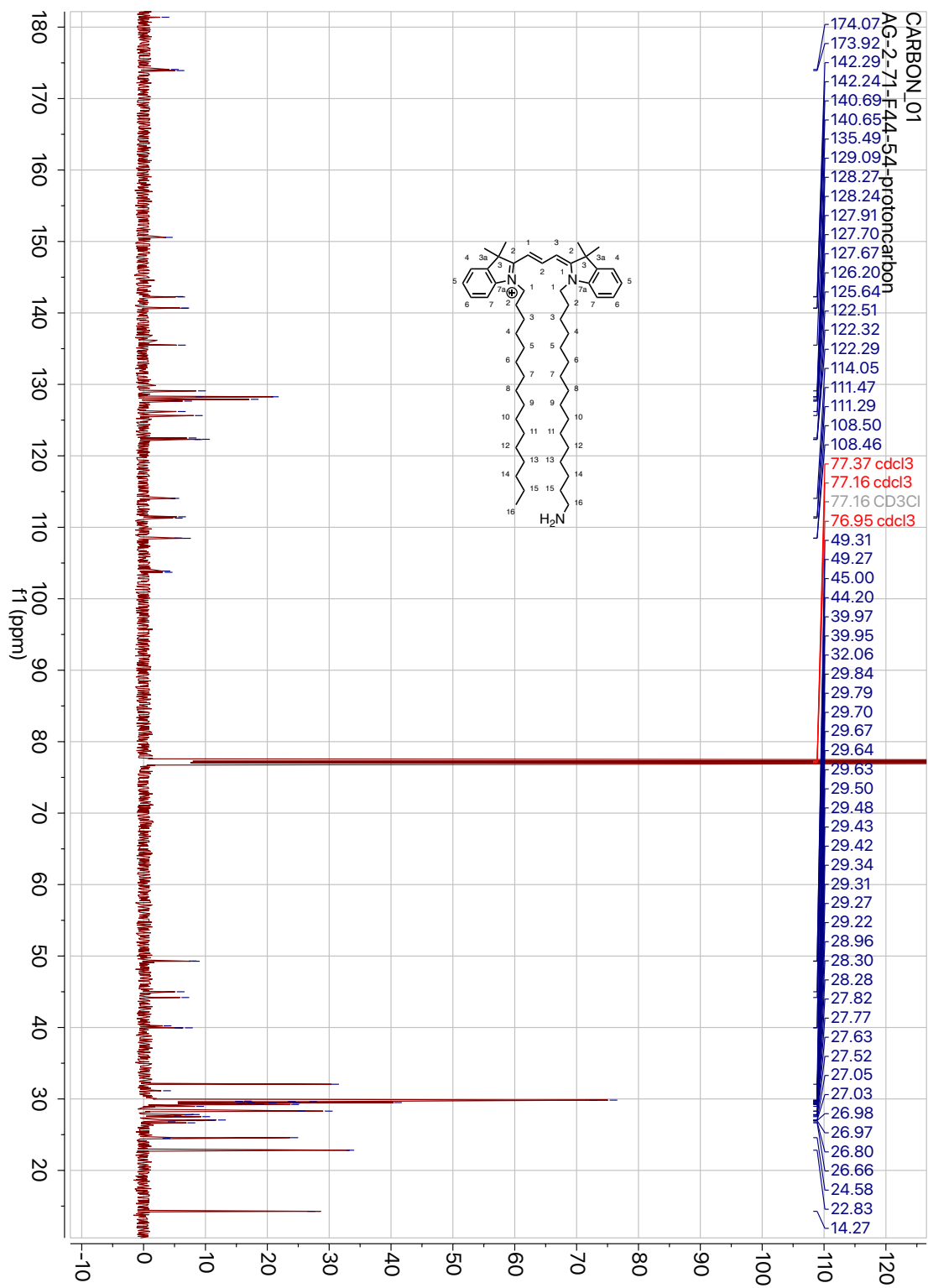
Compound 11: ¹³C NMR



Compound 12: H¹ NMR



Compound 12: ^{13}C NMR



¹³C NMR: DiIC₁₆TCO (2)

